ELSEVIER

Journal of Alloys and Compounds 404–406 (2005) 604–608

Journal of ALLOYS AND COMPOUNDS

www.elsevier.com/locate/jallcom

In situ SR-XRD studies of hydrogen absorption–desorption in $LaNi_{4.7}Sn_{0.3}$

M. Stange[a], J.P. Maehlen[a], V.A. Yartys[a,*], P. Norby[b], W. van Beek[c], H. Emerich[c]

[a] *Institute for Energy Technology, P.O. Box 40, Kjeller N-2027, Norway*
[b] *Department of Chemistry, University of Oslo, P.O. Box 1033, Blindern, N-0315 Oslo, Norway*
[c] *European Synchrotron Research Facility (ESRF), BP 220, F-38043 Grenoble, France*

Received 6 September 2004; accepted 5 January 2005
Available online 1 August 2005

Abstract

Phase-structural transformations during hydride formation and decomposition in the advanced hydrogen storage alloy $LaNi_{4.7}Sn_{0.3}$, are studied by in situ synchrotron X-ray powder diffraction (SR-XRD). A specially designed cell for in situ studies in H_2-atmosphere is attached to a metal hydride hydrogen storage unit developed at IFE providing hydrogen gas at convenient pressures. The studied sample is kept in a quartz glass capillary. Temperature cycling between RT and 100 °C at H_2 pressures of 2–3 bar was employed to $LaNi_{4.70}Sn_{0.30}H^{\circ}_{\sim 6}$ which resulted in a reversible hydrogen absorption–desorption process. Both a large temperature-dependent homogeneity range of the β-hydride and a small hysteresis in the formation-decomposition of the β-hydride have been revealed.

Keywords: Hydrogen storage materials; Diffraction; Synchrotron radiation

1. Introduction

$LaNi_5$-related hydrides have a wide range of applications including hydrogen storage and compression, H_2 purification and separation, heat management and nickel-metal hydride batteries [1–3]. The convenient properties of $LaNi_5$ include: a desorption pressure slightly exceeding 1 bar at room temperature, considerably fast absorption and desorption kinetics and easy activation [4,5]. A problem with pure $LaNi_5$, however, is that after cycling its hydrogen absorption–desorption properties are partially deteriorated which goes in parallel with loss of crystallinity evidenced by a significant line broadening [6]. After further cycling of the material, additional problems with disproportionation and reduced storage capacity appear [7].

$LaNi_5$ crystallizes in the $CaCu_5$-type structure (space group *P6/mmm*; 1 La in 1*a*: 0, 0, 0; 2 Ni1 in 2*c*: 1/3, 2/3, 0; 3 Ni2 in 3*g*; 1/2, 0, 1/2). Doping of $LaNi_5$ by different A and B elements can dramatically improve cycle life of the alloys and reduce the problem with hysteresis, peak broadening and intrinsic degradation. One successful example is $LaNi_{4.7}Sn_{0.3}$ where the B element Ni is substituted by Sn. $LaNi_{4.7}Sn_{0.3}$ is very attractive for the negative electrode in Ni–MH batteries. A lowering of the plateau pressure and a decrease in hydrogen capacity is observed with increasing Sn content [8]. From an applied point of view, it is also important that small Sn levels ensure a single-step formation and decomposition of the β-hydride preventing the formation of the intermediate $LaNi_5H_{\sim 3}$ (γ-phase) [9].

In situ synchrotron X-ray powder diffraction (SR-XRD) and powder neutron diffraction (PND) can provide important information on metal hydrides during the processes of hydrogen absorption and desorption. The data concerning mechanisms of phase-structural transformations during hydride formation, decomposition of metal hydrides and, furthermore, kinetic data for the absorption/desorption processes in "fast" intermetallic hydrides like $LaNi_5H_6$, can be obtained. In this contribution, $LaNi_{4.7}Sn_{0.3}$–H was studied with SR-XRD on temperature cycling between RT and 100 °C under H_2 pressures between 2 and 3 bar

* Corresponding author. Tel.: +47 63 80 64 53; fax: +47 63 81 29 05.
E-mail address: volodymyr.yartys@ife.no (V.A. Yartys).

0925-8388/$ – see front matter © 2005 Elsevier B.V. All rights reserved.
doi:10.1016/j.jallcom.2005.01.124

using a specially designed cell [10,11] for in situ studies in controlled environment (H_2 pressure/vacuum/temperature). For previous successful experiments on, e.g., hydrothermal conversion of zeolites using this cell, please see [10,11]. Focus here is to study the details of the development of the α- and β-phases during loading and release of hydrogen. Present work will make grounds for time-resolved SR-XRD studies of the absorption/desorption process aiming at getting information of the kinetics of hydrogen absorption and desorption in $La_{1-x}Mm_xNi_{5-y}Sn_y$; $x = 0$, 0.5, $y = 0$–0.4. In addition, ex situ diffraction data of original and hydrogen cycled alloy, with focus on studies of the line-broadening phenomenon, are described in this paper.

2. Experimental

$LaNi_{4.7}Sn_{0.3}$ was prepared by argon arc melting of a stoichiometric mixture of the elements La, Ni and Sn (>99.9 at.%). From an X-ray diffraction study, annealing at 950 °C for 1 week resulted in a single-phase material with $a = 5.06077(4)$ Å, $c = 4.02970(4)$ Å and $V = 89.38(2)$ Å^3 [12]. A detailed description of the sample preparation is given elsewhere [12].

Prior to the in situ SR-XRD experiments, the sample was activated by heating to 350 °C in dynamic vacuum and cooled to RT. Subsequent absorption/desorption experiments were repeated until the absorption started instantly after admission of hydrogen to the sample and was completed within a few seconds. The hydrogen loading pressure was varied between 3 and 12 bar. After the last desorption all handling of the sample was done in an argon-filled glove box.

Ex situ diffraction data of the starting alloy $LaNi_{4.7}Sn_{0.3}$ was measured at the Swiss Norwegian Beamline (BM01B), ESRF to study the Sn and Ni distribution in the metal matrix. To monitor the absorption/desorption process of $LaNi_{4.7}Sn_{0.3}$, in situ SR-XRD experiments were performed (BM01B).

A setup designed for in situ studies of reactions in gas/vacuum [10,11] was used. A small amount of the sample is contained in a 0.5 mm quartz glass capillary and fills approximately 1–2 mm in the bottom of the capillary. The capillary is hermetically connected to the gaseous system using a carbon ferrule mounted in a *T*-piece, which, in turn, is attached to the goniometer head. A two stringed flow system makes it possible to change between hydrogen gas and vacuum during the experiment. Connection of the microreaction cell to the goniometer head restricted rotation of the sample. Thus, we have restricted analysis of the Rietveld refinements mainly to the information concerning the modifications of the unit-cell dimensions. During the experiments, hydrogen gas is supplied from a portable metal hydride storage unit developed at IFE, Kjeller ($La_{1-x}Mm_xNi_5$, plateau pressure 2.5–3 bar). Vacuum is created via a turbomolecular vacuum pump. Stainless steel tubes were used for the connections to prevent oxygen diffusion through the tubes during the experiments.

λ was determined to ∼0.50000 or 0.49391 Å from separate calibration measurements of a standard Si sample. The diffractometer is equipped with six counting chains, with an angular offset in 2θ of ∼1.1°. For the in situ measurements, in order to keep the counting time per scan as low possible, the detector bank is moved by 1.2° during one measurement and the data from the six different detectors are added using a data-binning program. Data were obtained in steps of 0.01 in 2θ. By applying such a procedure, one data set ($2\theta = 8.66$–$15.38°$) was collected in 2 min during the heating and cooling of the sample under hydrogen pressure.

In the experiments described below, $LaNi_{4.7}Sn_{0.3}H_x$ is heated/cooled between RT and 200 °C under vacuum or hydrogen atmosphere ∼ at a constant pressure supplied by the MH storage unit using a heater gun with an air flow. Fully hydrogenated $LaNi_{4.7}Sn_{0.3}$ was prepared by heating the sample in vacuum to 200 °C before switching to H_2-atmosphere and cooling to room temperature. Data from a desorption/absorption cycle between 20 and 100 °C was thereafter measured under continuous heating (heating/cooling rate of 1 °C/min; Δt between start of each scan = 2.5 min). The temperature difference between the start and finish of each scan, $\Delta T = 2.5$ °C, was sufficiently low and was considered as "constant" as it did not result in visible variations of the unit-cell parameters due to changes in H-content or thermal expansion/contraction.

Information regarding line broadening of $LaNi_{4.7}Sn_{0.3}$ as a result of application of 5 hydrogenation cycles was obtained from comparative analysis of conventional powder X-ray diffraction data of the virgin and hydrogen cycled alloys (used for the in situ SR-XRD experiments). The data was collected with a Siemens D5000 diffractometer in Bragg–Bretano reflection geometry using monochromatic Cu $K_{\alpha 1}$ radiation from a germanium primary monochromator. A Si standard was used for internal standard and for instrument calibration. Data were obtained in steps of $\Delta 2\theta = 0.015552°$ as defined by the position sensitive detector (PSD). Instrumental resolution specified as FWHM for Si(1 1 1) is ∼ 0.12°. Rietveld analysis of the powder neutron diffraction data was carried out using the GSAS software [13].

3. Results and discussion

The unit-cell dimensions for $LaNi_{4.7}Sn_{0.3}$ determined from ex situ SR-XRD data ($\lambda = 0.49391$ Å); $a = 5.06099(1)$ Å, $c = 4.02986(3)$ Å, $V = 89.390(1)$ Å^3 correspond well with previously published values for $LaNi_{4.75}Sn_{0.25}$ ($a = 5.065$ Å, $c = 4.025$ Å, $V = 89.5$ Å^3) [14]. Site occupations of Sn and Ni were refined. The refinements showed that Sn preferred the 3*g* site compared to a random $2c + 3g$ model. However, a small Sn occupancy in the 2*c* site could not be ruled out. The stoichiometry of the sample was constrained to the initial composition and the displacement factors for Ni and Sn, respectively, were kept equal.

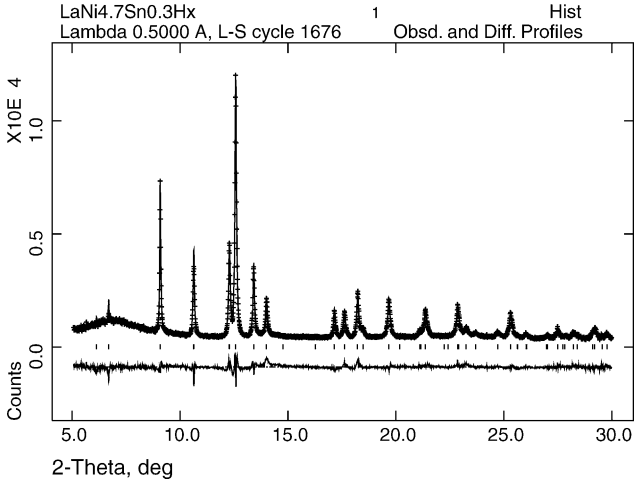

Fig. 1. SR-XRD pattern of $LaNi_{4.7}Sn_{0.3}H_{\sim 6}$ showing observed (+), calculated (line) and difference (bottom line) plots. The peak positions are marked by vertical lines.

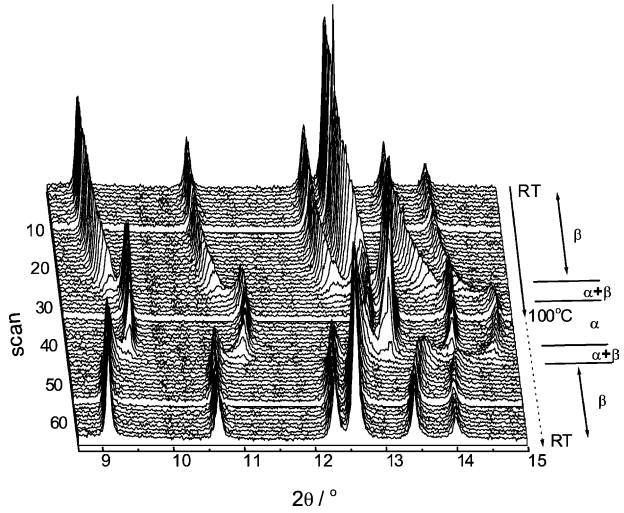

Fig. 2. Powder diffraction profiles during transformation of β-phase to α-phase on heating the saturated with hydrogen sample from 25 to 100 °C in H_2 gas and subsequent cooling to 25 °C to form back the β-phase.

Further analysis of SR-XRD and powder neutron diffraction data are planned to conclusively determine the Sn and Ni distribution.

Synthesis of the $LaNi_{4.7}Sn_{0.3}$-based β-hydride was achieved by applying the following procedure. The pre-activated $LaNi_{4.7}Sn_{0.3}$ was heated under vacuum to 200 °C before switching to hydrogen atmosphere ($pH_2 \sim 2.6$ bar) and cooling in H_2 to 25 °C. Refinement of the unit-cell dimensions of the collected in situ data showed that $LaNi_{4.7}Sn_{0.3}H_x$ reached a complete saturation with hydrogen. This conclusion is reached on the basis of comparison of the unit-cell parameters from the Rietveld refinements [$a = 5.3944(1)$ Å, $c = 4.2813(2)$ Å, $V = 107.89(1)$ Å^3] (see Fig. 1) and the reference data for $LaNi_{4.75}Sn_{0.25}H_{6.1}$ [14]; $a = 5.41$ Å, $c = 4.29$ Å and $V = 108.5$ Å^3. The observed H-induced volume increase, $\Delta V/V$, is 21.1% both for $LaNi_{4.75}Sn_{0.25}$ [14] and $LaNi_{4.70}Sn_{0.30}$. Hydrogen content H/$LaNi_{4.7}Sn_{0.3}$ estimated from comparison of the measured volume effects and literature data, is close to 6 at.H/f.u.

The hydride sample was cycled between 20 and 100 °C in H_2 gas. The cycling resulted in β↔α transformations during hydrogen release from $LaNi_{4.70}Sn_{0.30}H_{\sim 6}$ and loading of the α-phase by H_2. Fig. 2 shows the development of the powder diffraction profiles during hydrogen desorption and absorption. At the applied pressure of 2.6 bar H_2, the β-phase decomposes in the T-range ~ 82.5–92.5 °C and forms back from α-phase between 70 and 80 °C. This difference is caused by application of not completely equilibrium conditions of the experiment; such type of conditions is anticipated during hydrogen loading/unloading in an MH hydrogen storage unit. A complete reversibility of the transformations was achieved on cycling. Unit-cell dimensions in the single-phase regions as determined by Rietveld refinements are shown in Fig. 3.

The β-phase appears to have a large homogeneity range, most evidently seen from the variation along c ($\Delta c/c = -2.5\%$; $\Delta a/a = -1.2\%$; $\Delta V/V = -5.0\%$ between 20 and 82.5 °C). A small hysteresis in the unit-cell dimensions takes place between hydrogen absorption and desorption which again is more pronounced along c [0.09% along a versus 0.28% along c at 60 °C]. Both solubility range and hysteresis of the α-phase are significantly smaller than for β. The change

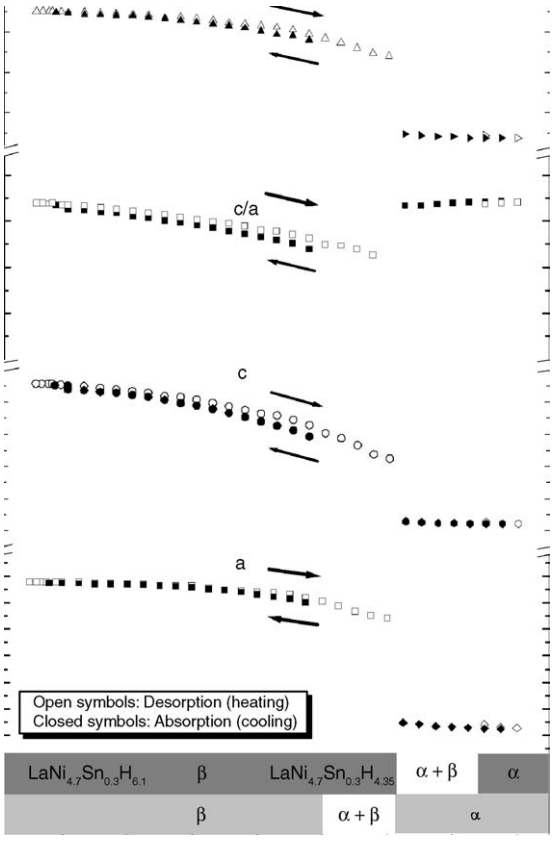

Fig. 3. Variations of the unit-cell dimensions of β-hydride and α-phase as a function of temperature.

in unit-cell dimensions is slightly more pronounced along a ($\Delta a/a = -0.12\%$; $\Delta c/c = -0.06\%$; $\Delta V/V = -0.30\%$). The homogeneity range of α is larger on absorption than during desorption while that of β is smaller.

The thermal expansion of $LaNi_{4.7}Sn_{0.3}$ during heating in vacuum over the same temperature range, 20–100 °C, was measured for a reference. This measurement yielded the values $\Delta c/c = 0.3\%$; $\Delta a/a = 0.4\%$; $\Delta V/V = 1.0\%$ and led to the conclusion that the effects caused by changes in hydrogen solubility dominate the behavior of the material and that the contribution from the thermal expansion/contraction effect is significantly weaker.

By disregarding the temperature-dependent unit-cell changes in the rather narrow temperature window, the reduction in unit-cell-volume of β corresponds to a homogeneity range of approximately $LaNi_{4.70}Sn_{0.30}H_{\sim 6.1–4.6}$ between 20 and 82.5 °C. The homogeneity range of α around 100 °C in H_2-atmosphere is very small judging from the small changes in unit-cell dimensions.

Complex transformations take place in the material in the area between the single-phase regions of the diagram. An α + β model with constant unit-cell dimensions over the multiphase region, was considered as oversimplified as it did not provide satisfactory description of the data collected. Because of that, the unit-cell dimensions in the multiphase regions are not included in Fig. 3. The appearance of an intermediate hydride related to $LaNi_5H_3$ [15] was considered and ruled out since none of the phases had unit-cell dimensions (c/a ratios) matching that of $LaNi_5H_3$ ($c/a = 0.7669$ [15]). This agrees with the reference data for the related Sn substituted $LaNi_5$-based hydrides where an intermediate hydride was not observed and so far regarded as one of the most important reasons for the increased cycling stability of $LaNi_{5-x}Sn_xH_y$ [16] compared to $LaNi_5$.

The experimental observations of this work allow a suggestion that the time resolution of the data is not sufficiently high to explain the phase transformations in the area of phase transformations. Further studies with a time interval of 3–5 s for each collected data set allowing to resolve the problem, are planned. A variation of the unit-cell dimensions over the two-phase region and a formation of new phases could be extra factors, which should be considered to explain the transformations. A possible inhomogenous distribution of hydrogen in the sample is also possible.

Finally, to study the effect of hydrogen cycling on the line widths of $LaNi_{4.70}Sn_{0.30}$, experimental half widths of selected reflections (conventional PXD data; Cu $K\alpha_1$; FWHM normalized with selected Si-reflections) of $LaNi_{4.70}Sn_{0.30}$ (annealed at 950 °C) were compared to those of the pre-cycled sample (exposed to 5 cycles in hydrogen). The line broadening is most likely related to the creation of lattice defects and microstrain [7] or partially caused by a non-complete release of hydrogen during cycling at RT. A significant broadening of the diffraction peaks (approximately doubling of the FWHM for the (1 1 0) reflection) is observed after cycling. This observation does not agree with the conclusion of [17] claiming that upon substitution of Ni by Sn in $LaNi_{5-x}Sn_x$ this effect vanishes for $x \geq 0.20$.

4. Conclusions

Hydrogen absorption/desorption properties of the $LaNi_{4.7}Sn_{0.3}$ intermetallic alloy, which is a prospective material for a wide range of applications, have been successfully studied using in situ SR-XRD in controlled gaseous and temperature environments. The results can be summarized as follows:

(i) The β-hydride has a large homogeneity range from 4.6 to 6.1 at.H/f.u. $LaNi_{4.7}Sn_{0.3}$;
(ii) A small hysteresis effect takes place between hydrogen absorption and desorption;
(iii) The region of phase-structural transformations α↔β is very complex and a high time-resolution of the in situ studies is required to uncover its mechanism.

Acknowledgements

This work received financial support from the Norwegian Research Council. We thank R.V. Denys (PhMI NAS Ukraine) for help in preparation of the alloy.

References

[1] P. Dantzer, H. Wipf (Eds.), Hydrogen in Metals. III. Properties and Applications (Topics in Applied Physics), vol. 73, Springer-Verlag, 1997, p. 279.
[2] T. Sakai, H. Yoshinaga, H. Miyamura, N. Kuriyama, H. Ishikawa, J. Alloys Comp. 180 (1992) 37.
[3] T. Sakai, M. Matsuoka, C. Iwakura, K.A. Gschneider Jr., L. Eyring (Eds.), Handbook on the Physics and Chemistry of Rare Earth, vol. 21, Elsevier Science, Amsterdam, 1995, Chapter 142, p. 133.
[4] J.S. Cantrell, T.A. Beiter, R.C. Bowman Jr., J. Alloys Comp. 207–208 (1994) 372.
[5] S.W. Lambert, D. Chandra, W.N. Cathey, F.E. Lynch, R.C. Bowman Jr., J. Alloys Comp. 187 (1992) 113.
[6] Y. Nakamura, K. Oguro, I. Uehara, E. Akiba, J. Alloys Comp. 298 (2000) 138.
[7] R.C. Bowman Jr., C.H. Luo, C.C. Ahn, C.K. Witham, B. Fultz, J. Alloys Comp. 217 (1995) 185.
[8] J.-M. Joubert, M. Latroche, R. Cerný, R.C. Bowman Jr., A. Percheron-Guégan, K. Yvon, J. Alloys Comp. 293–295 (1999) 124.
[9] S. Luo, W. Luo, J.D. Clewley, T.B. Flanagan, L.A. Wade, J. Alloys Comp. 231 (1995) 467.
[10] P. Norby, J. Am. Chem. Soc. 119 (1997) 5215.
[11] E. Krogh Andersen, I.G. Krogh Andersen, P. Norby, J.C. Hanson, J. Solid State Chem. 141 (1998) 235.
[12] O.Yu. Khyzhun, M.V. Lototsky, A.B. Riabov, C. Rosenkilde, V.A. Yartys, S. Jørgensen, R.V. Denys, J. Alloys Comp. 356 (2003) 773.
[13] A.C. Larson, R.B. Von Dreele, Program GSAS, General Structure Analysis Program, LANCE, MS-H 805, Los Alamos National Laboratory, Los Alamos, NM, USA.

[14] B. Fultz, C.K. Witham, T.J. Udovic, J. Alloys Comp. 335 (2002) 165.
[15] E. Akiba, H. Hayakawa, Y. Ishido, K. Nomura, S. Shin, Zeitschrift für Physicalische Chemie Neue Folge 163 (1989) 291.
[16] R.C. Bowman Jr., C.A. Lindensmith, S. Luo, T.B. Flanagan, T. Vogt, J. Alloys Comp. 330–332 (2002) 271.
[17] S. Luo, J.D. Clewley, T.B. Flanagan, R.C. Bowman Jr., L.A. Wade, J. Alloys Comp. 267 (1998) 171.